Nuclear Engineering and Technology 51 (2019) 207–213

Contents lists available at ScienceDirect

Nuclear Engineering and Technology

journal homepage: www.elsevier.com/locate/net

Original Article

Corrosion and mechanical properties of hot-rolled 0.5%Gd-0.8%B-stainless steels in a simulated nuclear waste treatment solution

Moo Young Jung [a], Youl Baik [a], Yong Choi [a], D.S. Sohn [b, *]

[a] Department of Materials Science and Engineering, Dankook University, Dandaer-ro 119, Cheonan, Chungnam 31116, Republic of Korea
[b] Department of Nuclear Engineering, UNIST, 50 UNIST-gil, Eonyang-eup, Ulju-gun, Ulsan 689-798, Republic of Korea

ARTICLE INFO

Article history:
Received 16 April 2018
Received in revised form
3 August 2018
Accepted 21 August 2018
Available online 10 September 2018

Keywords:
Gd-B-stainless steel
Corrosion
Neutron absorbing materials

ABSTRACT

Corrosion and mechanical behavior of the hot-rolled 0.5%Gd-0.8%B-stainless steel to develop a spent nuclear fuel storage material was studied in a simulated nuclear waste treatment condition with rolling condition. The austenite and ferrite phases of the 0.5%Gd-0.8%B-stainless steels are about 88:12. The average austenite and ferrite grain size of the plane normal to rolling, transverse and normal directions of the hot rolled specimens are about 5.08, 8.94, 19.35, 23.29, 26.00 and 18.11 [μm], respectively. The average micro-hardness of the as-cast specimen is 200.4 Hv, whereas, that of the hot-rolled specimen are 220.1, 204.7 and 203.5 [H_v] for the plane normal to RD, TD and ND, respectively. The UTS, YS and elongation of the as-cast and the hot-rolled specimen are 699, 484 [MPa], 34.0%, and 654, 432 [MPa] and 33.3%, respectively. The passivity was observed both for the as-cast and the hot rolled specimens in a simulated nuclear waste solution. The corrosion potential and corrosion rate of the as-casted specimens are −343 [mV_{SHE}] and 3.26×10^{-7} [A/cm^2], whereas, those of the hot rolled specimens with normal to ND, RD and TD are −630, −512 and −620 [mV_{SHE}] and 6.12×10^{-7}, 1.04×10^{-6} and 6.92×10^{-7} [A/cm^2], respectively. Corrosion tends to occur preferentially Cr and B rich area.

1. Introduction

Neutron shielding and absorbing materials have been attractive attention because of their important role in the long-time storage of spent nuclear fuels [1]. The neutron shielding and absorbing materials are composed of structural materials like stainless steels and neutron absorbers like boron. Borated stainless steels for neutron absorbing structural materials are common because of their high mechanical properties and excellent corrosion resistance.

Several researchers have investigated the corrosion performance and the general corrosion rates of the borated stainless steels [2]. The borated stainless steels performed similarly to conventional un-borated stainless steels in the condition of low chloride concentration and near-neutral pH. Increasing boron content and temperature increases corrosion rate that is at least four times that of the un-borated stainless steels [3]. No difference in corrosion resistance for stainless steel with 1.0–1.75% boron was observed in a spent fuel pool conditions of 68 °C and pH of 5.3 with 2000 ppm boric acid. Although currently available neutron shielding and absorbing materials for spent fuel storage are based on borated austenitic stainless steels, a problem such as reduced corrosion resistance and loss of boron by leaching during a long-term exposure in an acidic solution is reported [4]. Accordingly, a stainless steel with gadolinium is more challenging than other alloys for the long-term spent fuel storage with corrosion resistance. Recently, 0.5%Gd-0.8%B-stainless steels have been the most promising material for the long-term storage of spent nuclear fuel [5]. Because of their higher strength than any other alloys.

Although there are several results about the corrosion test of the stainless steels with gadolinium and boron, little information is available about the 0.5%Gd-0.8%B-stainless steel for a neutron shield and absorbing materials for a spent nuclear fuel storage, especially in nuclear waste treatment conditions. Hence, the objectives of this study are to fabricate the stainless steel with gadolinium and boron for neutron absorbers and to determine corrosion behavior in a simulated nuclear waste treatment condition.

* Corresponding author.
E-mail address: dssohn@unist.ac.kr (D.S. Sohn).

https://doi.org/10.1016/j.net.2018.08.017

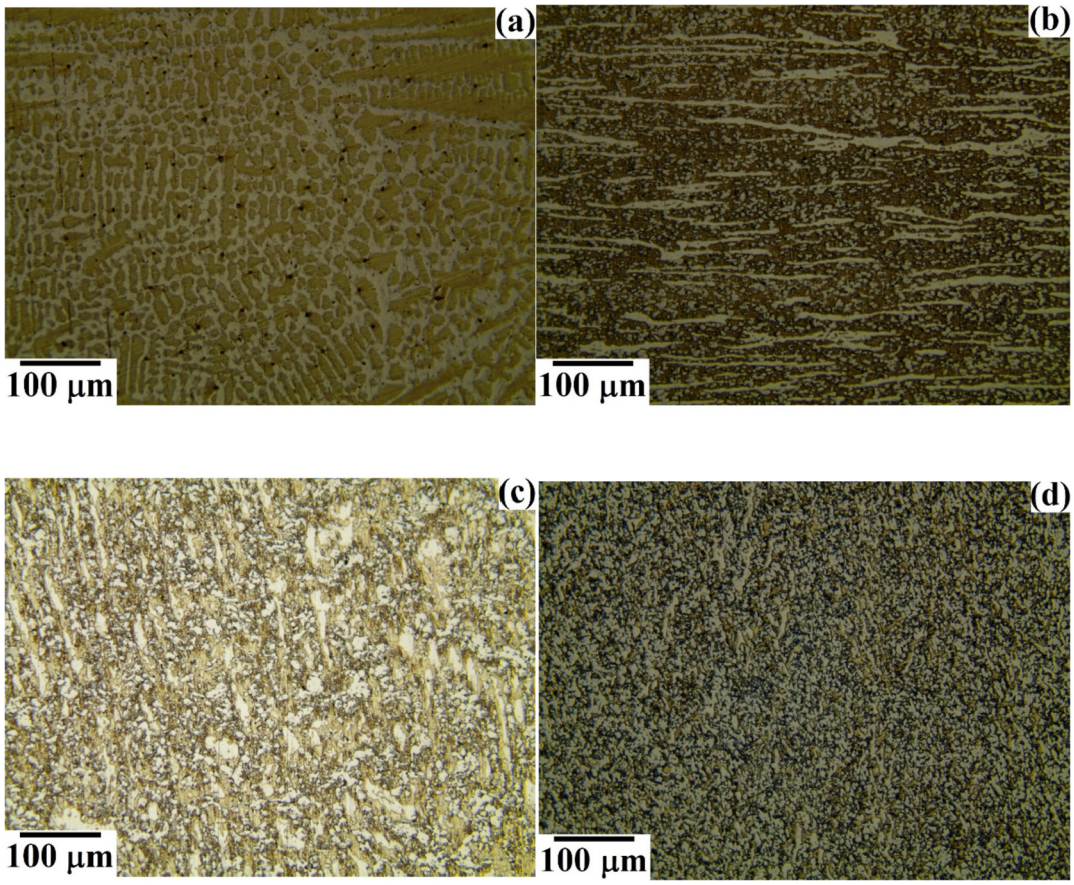

Fig. 1. The microstructures of 0.5%Gd-0.8%B-SUS316L alloy observed by optical microscope: (a)- microstructure of the as cast 0.5%Gd-0.8%B-SUS316L, (b), (c), (d)- microstructures of the hot-rolled 0.5%Gd-0.8%B-SUS316L with normal to TD, ND and RD.

Table 1
Average grain size of 0.5%Gd-0.8%B-SUS316L alloys [μm].

specimen	Austenite	Ferrite
As-cast	11.05 (2)	12.52 (2)
Rolled-RD⊥	5.08 (2)	8.94 (2)
Rolled-ND⊥	26.00 (2)	18.11 (2)
Rolled-TD⊥	19.35 (2)	23.29 (2)

2. Experimental method

2.1. Sample preparation

A cylindrical pellet with the composition of 0.5%Gd-0.8%B-stainless steel was prepared by using SUS316L powders (99.8%, 10 μm, Metalplayer Co, Korea), gadolinium powders (99.9%, 10 μm, Metalplayer Co., Korea), boron powders(95%, 5 μm Metalplayer Co, Korea) under uni-axil pressure of 3000 MPa. The pellet was vacuum arc melted (Vacuum Arc Melting System, Seoul Vacuum Tech. Ltd, Korea) and poured into Y-mold. The as-cast specimens were hot rolled at 1000 °C~1100 °C with the reduction ratio of 25%. The hot rolling process was conducted with 8 pass from initial thick of 7.5 mm to the final thick of 3.6 mm.

2.2. Microstructure observation and hardness determination

The specimen was mounted by acrylic resin and polished by various emery papers from #220 to #2000 to observe the microstructures. Final polishing was performed by diamond abrasives (1 μm, R & B, Korea). The specimens were etched by Kalling's etching solution (5 ml nitric acid + 100 ml ethanol) within 30 s. Microstructure was observed with an optical microscope (BX-53MRF-S, Olympus, Japan) at the planes normal to rolling (RD), normal (ND) and tangential directions (TD) respectively. Evaluation of grain sizes was investigated with ASTM E−112-13. Micro hardness of specimens was determined with Micro-vickers hardness tester(DHV-1000, Hautec, China) at 1 kgf loading within 15 seconds.

Table 2
Micro-vickers hardness and the UTS, YS and Elongation values.

Specimen		Micro Hardness [HV]	UTS [MPa]	YS [MPa]	Elongation [%]
As-cast		200.4 (1)	699.0 (1)	484.0 (1)	34.0 (1)
Hot-rolled	ND⊥	203.5 (1)	654.0 (1)	432.0 (1)	33.3 (1)
	RD⊥	220.1 (1)			
	TD⊥	204.7 (1)			

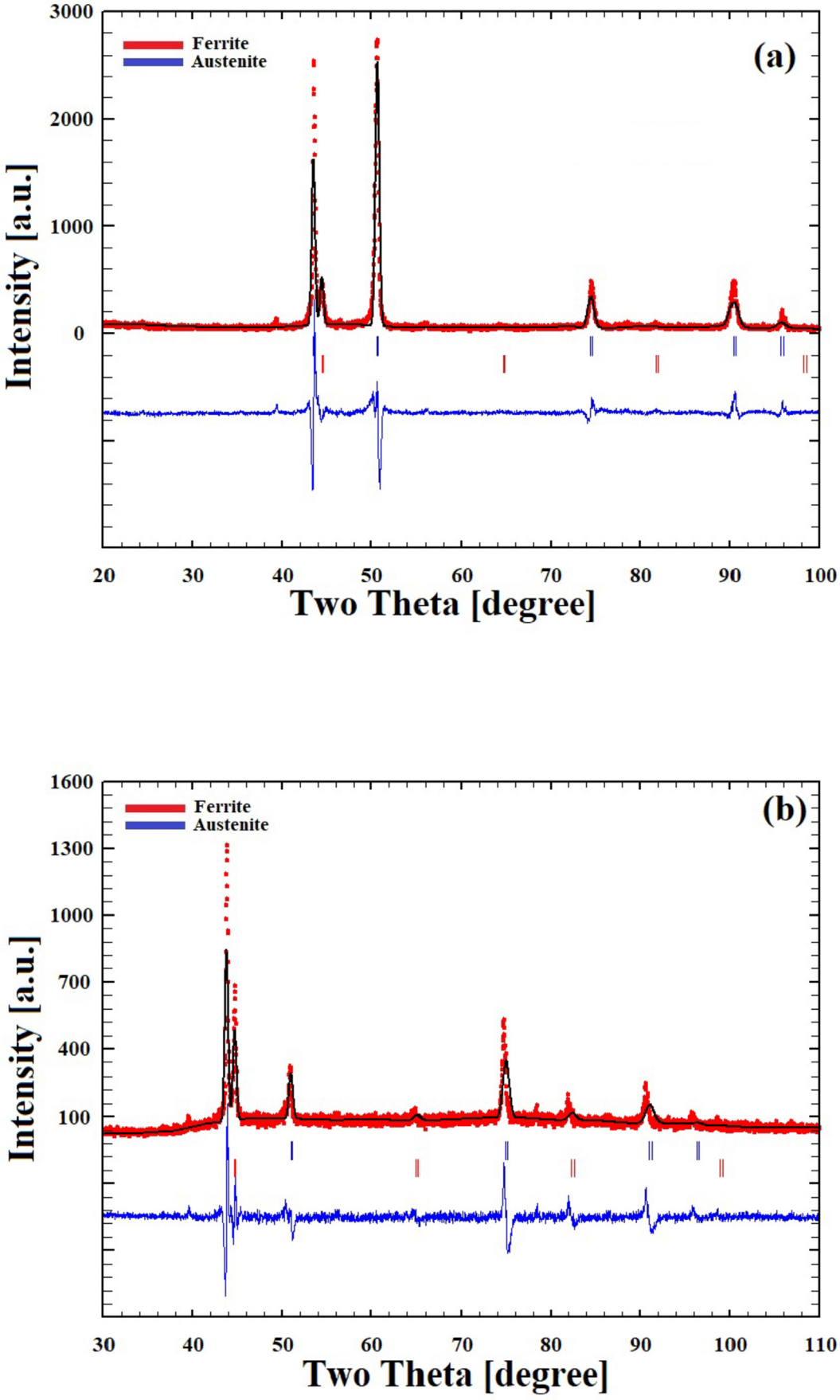

Fig. 2. XRD spectra of 0.5%Gd-0.8%B-SUS316L alloys: (a)- as-cast (b)- hot rolled.

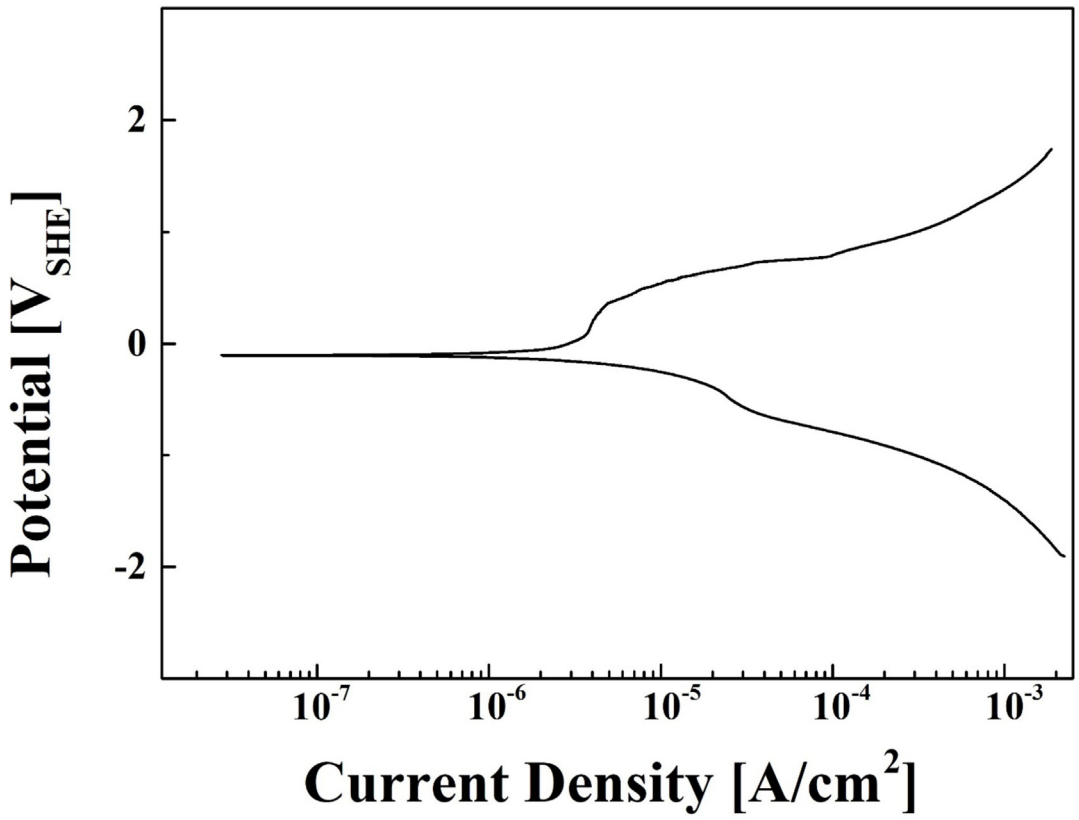

Fig. 3. Polarization curve of the as-cast 0.5%Gd-0.8%B-SUS316L.

2.3. Phase identification

Phase identification was carried out with a X-ray diffractometer (Ultima IV, Rigaku, Japan) at the condition of the diffraction angle from 30° to 100°, speed of 0.02°/sec, and Cu·Kα line at room temperature. Rietveld refinement was conducted by Fullprof 2014(ILL, France).

2.4. Corrosion test

Electrochemical corrosion test was performed with a Potentiostat (Zive Lab, ZIVE-BP2, Korea) in the simulated nuclear waste solution at room temperature. The counter and reference electrodes were a platinum wire and saturated calomel electrode (SCE), respectively.

3. Results and discussion

3.1. Microstructure observation and hardness determination

Fig. 1 is the microstructures of as-casted and hot rolled 0.5%Gd-0.8%B-stainless steel alloy observed by optical microscopy. As shown in Fig. 1-(a), typical dendritic structure was observed in the as-cast specimen, whereas, texture with the aspect ratio of more than two was clearly observed in the hot-rolled specimen in Fig. 1-(b), (c) and (d). This differences between them is due to plastic deformation caused by rolling process. Table 1 is the average grain size of austenite and ferrite with as-cast and hot rolled specimens. The average austenite and ferrite grain size of the as-cast specimen is about 11.05 [μm] and 12.52 [μm], respectively. The average austenite and ferrite grain size of the plane normal to transverse, normal and rolling directions of the hot rolled specimen in Fig. 1-(b), (c) and (d) are about 19.35, 23.29, 26, 18.11, 5.08, and 8.94 [μm], respectively. The maximum aspect ratio of about 2.3 was observed on the plane normal to transverse direction.

Table 2 is micro-vickers hardness and the UTS, YS and Elongation values. The average micro-hardness of the as-cast specimen is 200.4 Hv, whereas, that of the hot-rolled specimen are 220.1, 204.7 and 203.5 [H_v] for the plane normal to RD, TD and ND, respectively. The increased hardness is related to grain size refinement and work hardening. Since the grain size refinement is proportional to the square root of the grain size, the increased hardness of the hot-rolled specimen is expected to be mainly due to grain size refinement without any other hardness mechanisms like work hardening effects. The UTS, YS and elongation of the as-cast and the hot-rolled specimen are 699 MPa, 484 MPa, 34.0%, and 654 MPa, 432 MPa and 33.3%, respectively.

3.2. Phase identification

Fig. 2 is the X-ray spectra of the as-cast and the hot rolled-0.5% Gd-0.8%B-stainless steels. As shown in Fig. 2, main phases are austenite and ferrite phases. Rietveld refinement shows that the austenite and ferrite phases of the as-cast and the hot-rolled 0.5% Gd-0.8%B-stainless steels are 92.40(4.62): 7.60(1.00) [$\chi^2 = 5.62$], and 76.23(3.81): 23.77(1.00) [$\chi^2 = 4.18$], respectively. It is difficult to observe gadolinium and boron compounds, which means that those elements exist as solid solution [6]. The reason why increased ferrite phase of the hot rolled 0.5%Gd-0.8%B-stainless steels is the heat effect [7].

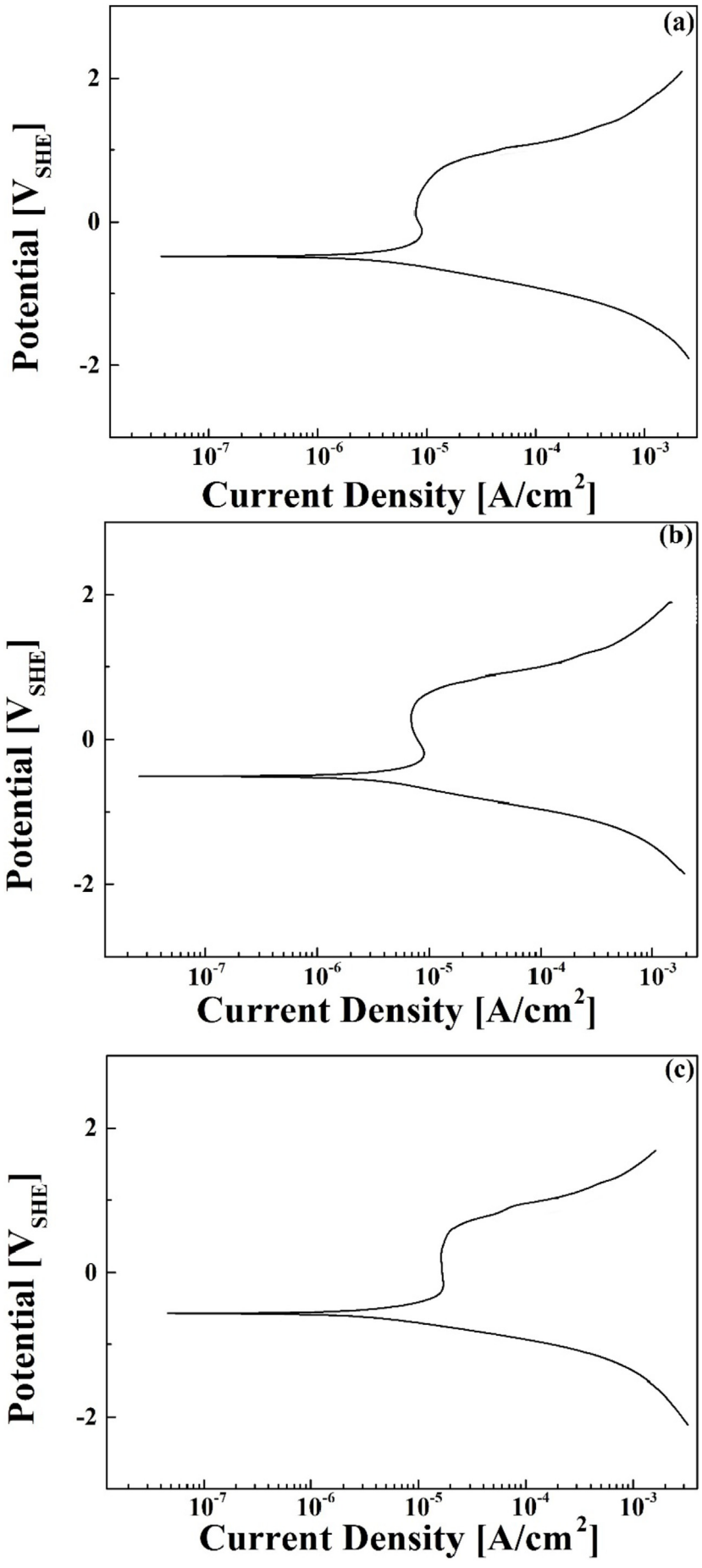

Fig. 4. Polarization curves of the hot rolled 0.5%Gd-0.8%B-SUS316L with normal to (a)ND, (b)RD, (c)TD.

Table 3
The corrosion potential and corrosion rate of 0.5%Gd-0.8%B-SUS316L alloys with as cast and hot rolled conditions.

Specimen		E_{corr} [mV_{SHE}]	I_{corr}[A/cm^{-2}]
As-cast		−343.0 (1)	3.26×10^{-7}
Hot-rolled	ND⊥	−630.0 (1)	6.12×10^{-7}
	RD⊥	−512.0 (1)	1.04×10^{-6}
	TD⊥	−620.0 (1)	6.92×10^{-7}

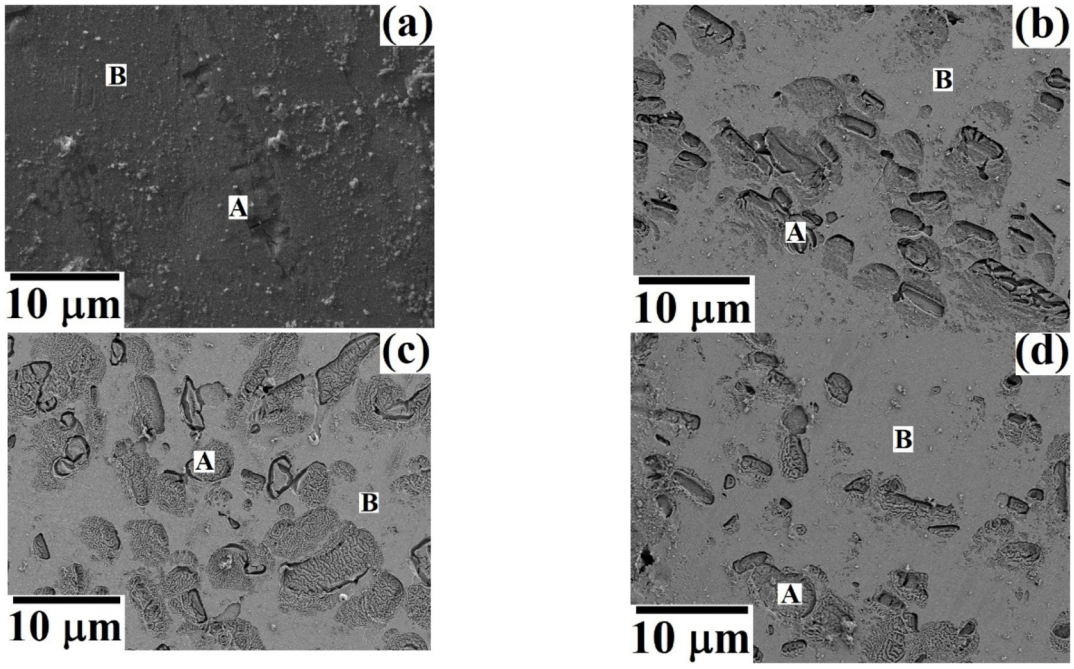

Fig. 5. SEM images of the surfaces after corrosion test with (a)as-cast and plane normal to (b)TD, (c)ND, (d)RD.

3.3. Electrochemical corrosion test

Figs. 3 and 4 are polarization curves of the as-cast and the hot rolled specimens in a simulated nuclear waste solution, in which the passivity is clearly observed near the potential of 100 mV_{SHE} for the as-cast specimen and −100 mV_{SHE} for the hot-rolled specimens. Table 3 is the corrosion potential and corrosion rate of the as-cast and the hot rolled specimens. As shown in Table 3, those of the as-casted specimens are −343 [mV_{SHE}] and 3.26×10^{-7} [Acm^{-2}], whereas, those of the hot rolled specimens with normal to ND, RD and TD are −630, −512 and −620 [mV_{SHE}] and 6.12×10^{-7}, 1.04×10^{-6} and 6.92×10^{-7} [Acm^{-2}], respectively. The as-cast specimen has higher corrosion resistance than the hot-rolled specimen. In case of the hot-rolled specimen, as shown in Fig. 4, and Tables 1 and 3, the corrosion rate is the fast at the surface normal to rolling direction. The average grain size of the hot rolled specimens increase in the order of the surface normal to rolling, transverse and short-transverse directions. It means that the high corrosion rate at the surface normal to the rolling direction is relative to large grain boundary effect.

Table 4
The composition variation of the corroded surfaces obtained by EDX [wt.%].

Element Position	B	Cr	Gd	Fe	Ni
A	67.29 (2)	31.06 (2)	0.09 (2)	1.56 (2)	0.00 (2)
B	57.39 (2)	3.09 (2)	0.08 (2)	39.43 (2)	0.00 (2)

Fig. 5 shows the SEM images of the surfaces after corrosion test with (a)as-cast and plane normal to (b)TD, (c)ND, (d)RD specimens. As shown in Fig. 5, the surface cracks due to corrosion were clearly obtained. The spots marked with A and B in Fig. 5 are the different amount of the failed areas by corrosion, respectively. Table 4 is the compositions of the corroded surface analyzed by EDX. As shown in Table 4, much more Cr and B are present at the area marked A, whereas more Fe at area marked B in Fig. 5. This means that corrosion tends to preferentially occur at the Ct and B rich area. This is well agreement with previous [8].

4. Conclusions

(1) The average austenite and ferrite grain size of the as-cast specimen prepared in this study are about 15.2 [μm] and 12.52 [μm], respectively. The average austenite and ferrite grain size of the plane normal to rolling, transverse and normal directions of the hot rolled specimen are about 5.25, 8.94, 24.12, 23.29, 18.25, 18.11 [μm], respectively. The maximum aspect ratio of about 2.3 was observed on the plane normal to transverse direction.
(2) The average micro-hardness of the as-cast specimen is 200.4 Hv, whereas, that of the hot-rolled specimen are 220.1, 204.7 and 203.5 [H_V] for the plane normal to RD, TD and ND, respectively.
(3) The austenite and ferrite phases of the as-cast and the hot-rolled 0.5%Gd-0.8%B-stainless steels are 88.85:11.15, and 88.87:11.13, respectively.

(4) The corrosion potential and corrosion rate of the as-casted specimens are −343 [mV_{SHE}] and 3.26×10^{-7} [A/cm^2]. Whereas, those of the hot rolled specimens with normal to ND, RD and TD are −630, −512 and −620 [mV_{SHE}] and 6.12×10^{-7}, 1.04×10^{-6} and 6.92×10^{-7} [A/cm^2], respectively.
(5) The passivity was observed for the as-cast and the hot rolled specimens in a simulated nuclear waste solution. The corrosion potential and corrosion rate of the as-casted specimens are −343 [mV_{SHE}] and 3.26×10^{-7} [Acm^2], whereas, those of the hot rolled specimens with normal to ND, RD and TD are −630, −512 and −620 [mV_{SHE}] and 6.12×10^{-7}, 1.04×10^{-6} and 6.92×10^{-7} [Acm^2], respectively. The as-cast specimen has higher corrosion resistance than the hot-rolled specimen. Corrosion tends to occur preferentially Cr and B rich area.

Acknowledgement

This work was supported by the Nuclear Power Core Technology Program of the Korea Institute of Energy Technology Evaluation and Planning (KETEP), granted financial resources from the Ministry of Trade, Industry and Energy, Republic of Korea (No. 20141710201690).

References

[1] A. Van Konynenburg, P.G. Curtis, T.S.E. Summers, Scoping Corrosion Tests on Candidate Waste Package Basket Materials for the Yucca Mountain Project, Lawrence Livermore National Laboratory, 1998. UCRL-ID-130386.
[2] K. Lindquist, Handbook of Neutron Absorber Materials for Spent Nuclear Fuel Transportation and Storage Applications, 2006 Edition, EPRI, Palo Alto, CA, 2006, 2006, 1013721.
[3] G.W. Wachs, J.W. Sterbentz, W.L. Hurt, P.E. McConnell, C.V. Robino, F. Tovesson, T.S. Hill, Nickel-Based Gadolinium Alloy for Neutron Adsorption Application in Ram Packages, Miami, FL, 2007. INL/CON-07–13343.
[4] David V. Fix, John C. Estill, Lana L. Wong, Raul B. Rebak, General and Localized Corrsion of Austenitic and Borated Stainless Steels in Simulated Concentrated Ground Waters, ASME-Pressure Vessels and Piping, San Diego, CA, 2004. UCRL-PROC-202920.
[5] Yong Choi, Byung M. Moon, Dong-Seong Sohn, Fabrication of Gd containing duplex stainless steel sheet for neutron absorbing structural materials, Nuclear Engineering and Technology 45 (2013) 689–694.
[6] G. RajaKumar, G.D.J. Ram, S.R.K. Rao, Microstructure and mechanical properties of borated stainless steel (304B) GTA and SMA welds, La Metall. Ital. 5 (2015) 47.
[7] Sung-Yu Kim, Hyuk-Sang Kwon, Heesan Kim, Effect of delta ferrite on corrosion resistance of Type316L stainless steel in acidic chloride solution by micro-droplet cell, Solid State Phenom. 124–126 (2007) 1533–1536.
[8] N. Parvathavarthini, R.K. Dayal, H.S. Khatak, V. Shankar, V. Shanmugam, Sensitization behavior of modified 316N and 316L stainless steel weld metals after complex annealing and stress relieving cycles, J. Nucl. Mater. 355 (2006) 68–72.